INTEGRATION OF RENEWABLE ENERGY FOR POWER TRANSFER IMPROVEMENT OF THE NIGERIAN 330KV TRANSMISSION NETWORK

ABSTRACT

The Nigerian 330 kV transmission network faces challenges related to voltage instability and significant power losses, which impact its power transfer capability. This study, titled "Integration of Renewable Energy for Power Transfer Improvement of the Nigerian 330kV Transmission Network"**,** explores the integration of renewable energy sources as a means to address these challenges. 5-bus electricity grid is considered as a test network. The steady state performance of the system was modelled using Newton-Raphson load flow equations and was simulated without and with renewable energy sources on MATLAB/Simulink toolbox (version 'R2016a'). The obtained results showed that without renewable energy integration, four key buses (buses 2, 3, 4, and 5) in the test network exhibited voltage magnitudes outside the acceptable operational range of $0.95 \leq V_i \leq 1.05$ per unit, with respective voltages of 0.8302, 0.6338, 0.5344, and 0.6581 per unit. However, when renewable energy was incorporated, these buses saw a marked improvement in voltage stability, reaching values of 0.9902, 1.0001, 1.0100, and 0.9947 per unit, respectively, and achieving compliance with the acceptable range. Additionally, the integration resulted in a substantial reduction in total active power loss, from 3.05 MW to 0.65 MW, representing a 78.33% improvement. These findings demonstrate that renewable energy integration can enhance voltage stability, reduce power loss, and thereby increase the transmission network's power transfer capability. This study underscores the potential for renewable energy to support the reliability and efficiency of Nigeria's power infrastructure.

Keywords: transmission network, renewable energy, load flow analysis, modeling, simulink

1. INTRODUCTION

In the last twenty years, global power demand has seen a notable rise. As of 2023, electricity consumption in Nigeria exceeded 40 terawatt-hours, following a steady upward trend that began around 2020, with annual increases observed between 2010 and 2018 as well [1]. This demand surge can largely be attributed to the country's rapidly growing population. Despite this, more than 60 percent of Nigerians lacked access to electricity in 2022, due to limitations such as insufficient transmission infrastructure.

The expansion of Nigeria's power generation and transmission capabilities has been heavily restricted by high energy prices, environmental regulations, challenges in obtaining right-of-way, and the high expenses associated with constructing new generation plants and transmission lines [2]. Consequently, certain transmission lines are overloaded, affecting system stability and lowering the quality of power delivered to consumers [3, 4].

Additionally, population-driven increases in power demand have complicated network interconnections, leading to issues like voltage instability, power security concerns, blackouts, insufficient reactive power, and significant transmission losses over long

distances [3]. Nigeria's electricity supply system thus faces various operational difficulties, including poor power quality, voltage instability, and large transmission losses. Traditional methods to address these problems include the deployment of synchronous generators, series compensation capacitors, generator excitation controls, magnetically controlled reactors, system reconfiguration, and the strategic addition or removal of shunt and series capacitors.

While these techniques have proven effective in improving voltage and power stability [5, 6, 7], they are often hindered by slow response times and susceptibility to mechanical wear, making them less optimal for power transmission enhancement [5]. As a result, integrating renewable energy sources has emerged as a more economical and responsive alternative to traditional approaches [8]. Increasingly, renewable energy sources (RESs) are being adopted globally to meet rising energy demands sustainably and to reduce reliance on fossil fuels [9, 10, 11].

The transition to RESs is driven by climate change concerns, the need to lower carbon emissions, fluctuating fuel prices, and market instabilities [12]. Many countries now aim to establish near-zero emission power sectors, a goal that requires greater integration of renewable energy into the grid. Nations like Iceland have achieved 100% renewable energy (RE) grid penetration, Norway reached 98% in 2019, and Kenya and Brazil have surpassed 70% RE grid penetration [13].

Recently, many developed and developing countries have adopted renewable energy as a cleaner alternative to conventional, polluting energy sources [14, 15]. In the field of Renewable Energy Sources (RES), there are several options for harnessing sustainable power, including hydro, solar, wind, and geothermal energy [15]. Hydropower generation converts the energy of flowing water into electricity using hydraulic turbines and generators. Because of their rapid start-up capabilities, many countries consider HPPs a primary source for meeting electricity demands [8]. However, the initial capital investment required for hydropower plants (HPPs) is substantial. Solar power, harnessed from the sun, is the most abundant energy source available today. It is captured primarily through photovoltaic (PV) solar cells, which convert sunlight into electrical energy. These PV cells can be connected in various configurations to form panels, improving energy production efficiency. Additionally, solar collectors focus sunlight to generate steam, which drives turbines to produce electrical energy, a process known as concentrated solar thermal power (CSP) [16, 17].

Wind power plants (WPPs) convert wind energy into electricity through the rotation of blade-driven generators at adequate wind speeds. Wind power, a free and clean energy source, has been used for electricity generation since its inception in Denmark in 1890. Over time, wind power has evolved from generating small amounts of electricity to producing several megawatts. Today, large WPPs compete with other energy sources, offering economical and clean power worldwide [8, 18, 19] .

Although both solar and wind power systems are intermittent, they have the advantages of being free and environmentally friendly. The challenges posed by their intermittency can be mitigated through effective weather forecasting and energy storage systems, such as batteries [20, 21].

Geothermal systems work similarly to other steam turbine-driven systems, with the key difference being the source of steam, which comes from heat within the Earth. These systems generate steam through deep wells, which drives turbines connected to generators, producing electricity [22].

It is worth noting that renewable energy sources (RES) can be integrated into the grid at various voltage levels, depending on the technology and the power capacity of the plant. CSP, wind power, and small to medium hydropower can connect to the grid at transmission levels, typically between 145 kV and 400 kV [23].

The voltage level at the connection point is stabilized with adequate reactive power support. Despite Nigeria's considerable renewable energy potential especially in solar, wind, and hydropower development in these areas remains limited. Only hydropower has seen

substantial use, though its full potential has yet to be harnessed. Solar energy, on the other hand, is predominantly used by urban households and a few rural communities [24].
There is an urgent need for policies and strategies to harness Nigeria's abundant RES, which could significantly improve the power sector's performance and reliability [25, 26].

1.1 Role of Renewable Energy in the Nigerian Power System

Nigeria's electricity supply remains inconsistent, with minimal signs of improvement. This unreliable power supply negatively affects the manufacturing, service, and residential sectors, posing a barrier to the country's economic growth. Despite recent power sector reforms, over half of the population still lacks access to electricity [27]. This paper aims to outline potential solutions for Nigeria's electricity challenges by examining the power sector comprehensively and assessing the potential for renewable energy.

Nigeria is rich in resources such as solar radiation, wind energy, and hydropower, which could be integrated into its power system. This integration involves capturing energy from solar panels, wind turbines, and hydropower plants and feeding it into the national grid [28]. By introducing renewable energy sources, the energy mix within the Nigerian power system can be diversified, thereby reducing reliance on fossil fuels. This diversification enhances the system's resilience against fluctuations in fuel prices and potential supply disruptions [29] present.

In the context of promoting sustainable energy growth in Nigeria, a study discussed the benefits of a Grid-Connected (GC) Hybrid Power System (HPS) as a supplementary source of power to the grid. This study proposed optimal hybrid system configurations tailored to specific locations and compared them with off-grid configurations of similar setups based on technical and economic factors.
Moreover, the need for alternative energy sources that are sustainable has been emphasized in revamping Nigeria's economic sectors. Renewable energy is highlighted as a key factor in enhancing productivity across all sectors, aligning with sustainable development goals. The implementation of Nigeria's Renewable Energy Master Plan (REMP) is seen as crucial for competing on a global scale by 2030 [30].

Additionally, research examining the integration of Renewable Energy Sources (RES) with Smart Grid Technology (SGT) in Nigeria identified current electricity supply challenges and evaluated existing policies. It compared Nigeria's power network with those in other countries, pinpointing major issues and obstacles within the electricity sector. The study advocated for the incorporation of RES with SGT into the grid and provided significant policy recommendations to address barriers that could impede this integration [31]. The findings are valuable for policymakers and renewable energy developers in crafting effective strategies for smoothly incorporating renewable energy into Nigeria's electricity supply mix.

2. METHODOLOGY

Based on the flow chart, the process began with a literature review on the integration of renewable energy for improving power transfer on the transmission network. Following this, a mathematical expression was developed for bus modelling of the power system network. After the mathematical expression, a review was carried out again to choose a situation software for modelling and simulating and analyzing of the system. MATLAB/Simulink simulation software was chosen because it provides a comprehensive environment for modelling, simulating, and analyzing complex systems. It's also allowed for detailed modelling of the behavior of transmission network steady state condition as well as integrating seamlessly with other MATLAB toolboxes and software packages, enabling engineers to perform multidomain simulations and incorporate additional functionalities such

as signal processing, control system design, and optimization. The system for both transmission network and renewable energy source was modelled with appropriate functional block in Simulink library as presented in Fig. 1. The modelled transmission network was simulated, and a renewable energy source was integrated to enhance the power transfer capability of the transmission system.

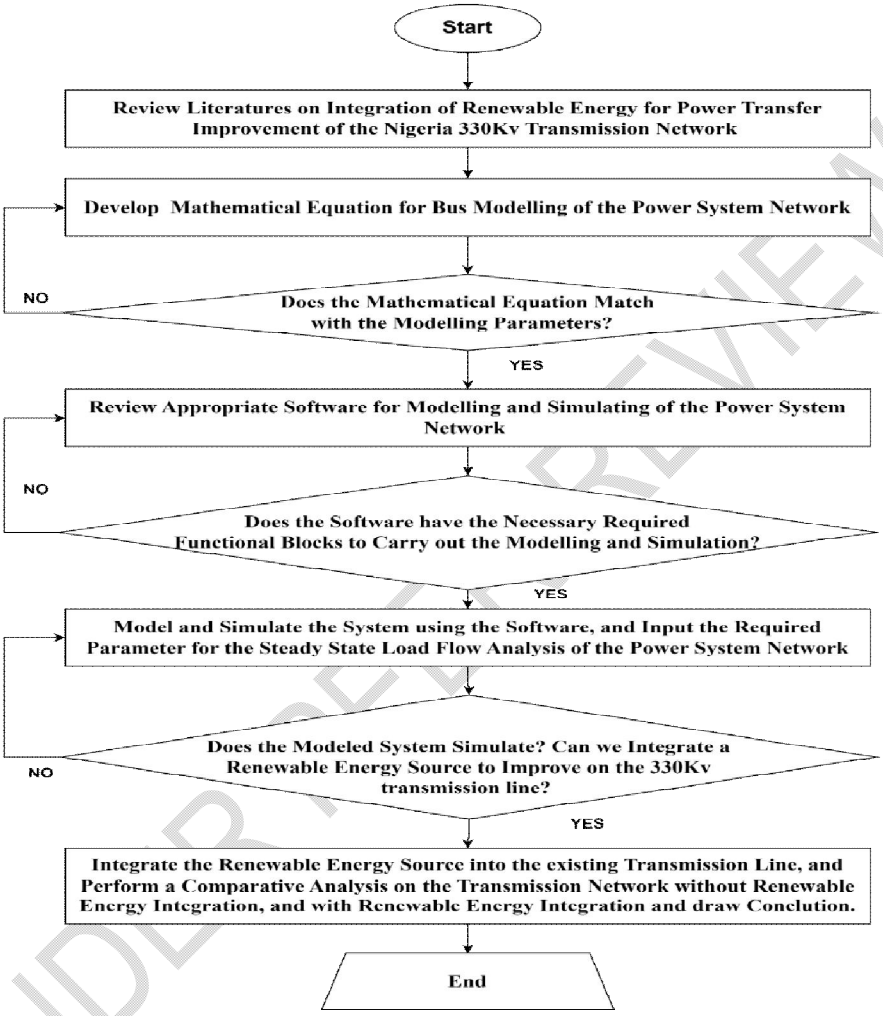

Fig. 1. Flow chart of the research paper

2.1 Load Flow Analysis

Load flow analysis serves as a highly effective tool for evaluating the performance of power systems. It provides essential data, including bus voltage magnitudes, phase angles, and the real and reactive power flows through transmission lines key factors in assessing system performance and considering future network enhancements [32]. Fig. 2 illustrates a typical model of the i^{th} bus within a power system network. By applying Kirchhoff's Current Law (KCL) to bus i and using Ohm's law for the connections between bus i and buses 1 through n, an expression for the current I_i injected at bus i^{th} can be derived. This is shown in equation (1)[33, 34].

$$I_i = \sum_{k=1}^{n} Y_{ik} V_k ; i, k = 1,2 \dots \dots \dots n \quad (1)$$

Where:

Y_{ik} = $Admittance\ between\ bus\ i\ and\ bus\ k$

V_k = Voltage at bus k

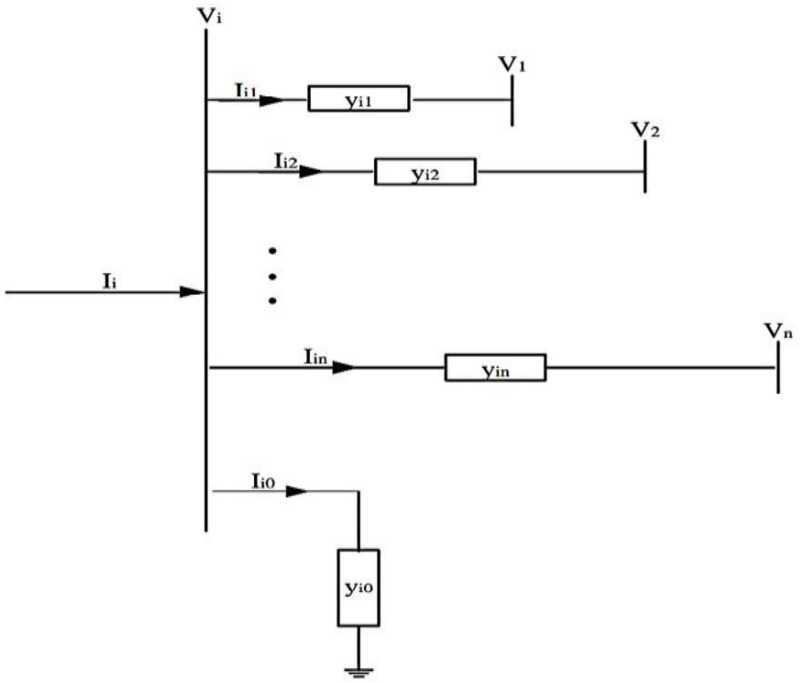

Fig. 2. A typical power system [33, 34]**.**

The complex apparent power injected by the source into the i^{th} bus can be expressed by the following equations: [33, 34].

$$S_i = P_i + jQ_i = V_i I_i^* ;\ i = 1,2 \dots \dots \dots n \quad (2)$$

Rearranging equation (2) to isolate the current I_i results in equation (3), which can be further transformed into equation (4) through straightforward cross multiplication.

$$I_i = \left(\frac{S_i}{V_i}\right)^* = \frac{P_i - jQ_i}{V_i^*} \quad (3)$$

$$P_i - jQ_i = V_i^* I_i \quad (4)$$

By substituting equation (1) into equation (4), we arrive at equation (5), from which the real and reactive powers are derived as expressed in equations (6) and (7).

$$P_i - jQ_i = V_i^* (\sum_{k=1}^{n} Y_{ik} V_k) ; i, k = 1,2 \dots \dots \dots n \quad (5)$$

$$P_i = Re(V_i^* (\sum_{k=1}^{n} Y_{ik} V_k)) \quad (6)$$

$$Q_i = -Im(V_i^* (\sum_{k=1}^{n} Y_{ik} V_k)) \quad (7)$$

To simplify the number of equations, $,V_i, V_i^*, V_k \; and \; Y_{ik}$ are represented in polar form as indicated in equations (8) to (11)[33]. Substituting equations (8) to (11) into equations (6) and (7) produces equations (12) and (13), respectively.

$$V_i = |V_i|e^{j\delta i} \tag{8}$$

$$V_i^* = |V_i^*|e^{j\delta i} \tag{9}$$

$$V_k = |V_k|e^{j\delta k} \tag{10}$$

$$Y_{ik} = |Y_{ik}|e^{j\theta_{ik}} \tag{11}$$

$$P_i = V_i^* \sum_{k=1}^{n} |Y_{ik}||V_k| \, G_{ik}\cos\theta_{ik} + \delta k - \delta i \tag{12}$$

$$Q_i = V_i^* \sum_{k=1}^{n} |Y_{ik}||V_k| \, B_{ik}\sin\theta_{ik} + \delta k - \delta i \tag{13}$$

Where:
$G_{ik} \; and \; B_{ik}$are the conductance and susceptance of the transmission line between buses $i \; and \; k$.
θ_{ik} are the voltage phase angles at buses$i \; and \; k$.
$|Y_{ik}||V_k$ are the voltage magnitudes at buses $i \; and \; k$.
Equations (12) and (13) are referred to as static load flow equations. These equations provide the steady-state solutions of the system and are typically non-linear, requiring various numerical methods for their solution. In this work, the Newton-Raphson iterative technique is employed due to its accuracy, reliability, and rapid convergence rate[33, 35, 34]. The Newton-Raphson load flow equations are represented by equation (14) and can be abbreviated as equation (15),[33, 35, 34].

$$\begin{bmatrix} \Delta P_2 \\ \Delta P_3 \\ \vdots \\ \Delta P_n \\ \Delta Q_2 \\ \Delta Q_3 \\ \vdots \\ \Delta Q_n \end{bmatrix} = \begin{bmatrix} \frac{\partial P_2}{\partial \delta_2} \frac{\partial P_2}{\partial \delta_3} \cdots \frac{\partial P_2}{\partial \delta_n} \frac{\partial P_2}{\partial V_2} \frac{\partial P_2}{\partial V_3} \cdots \frac{\partial P_2}{\partial V_n} \\ \frac{\partial P_3}{\partial \delta_2} \frac{\partial P_3}{\partial \delta_3} \cdots \frac{\partial P_3}{\partial \delta_n} \frac{\partial P_3}{\partial V_2} \frac{\partial P_3}{\partial V_3} \cdots \frac{\partial P_3}{\partial V_n} \\ \vdots \quad \vdots \quad \vdots \quad \vdots \quad \vdots \quad \vdots \quad \vdots \quad \vdots \\ \frac{\partial P_n}{\partial \delta_2} \frac{\partial P_n}{\partial \delta_3} \cdots \frac{\partial P_n}{\partial \delta_n} \frac{\partial P_n}{\partial V_2} \frac{\partial P_n}{\partial V_3} \cdots \frac{\partial P_n}{\partial V_n} \\ \frac{\partial Q_2}{\partial \delta_2} \frac{\partial Q_2}{\partial \delta_3} \cdots \frac{\partial Q_2}{\partial \delta_n} \frac{\partial Q_2}{\partial V_2} \frac{\partial Q_2}{\partial V_3} \cdots \frac{\partial Q_2}{\partial V_n} \\ \frac{\partial Q_3}{\partial \delta_2} \frac{\partial Q_3}{\partial \delta_3} \cdots \frac{\partial Q_3}{\partial \delta_n} \frac{\partial Q_3}{\partial V_2} \frac{\partial Q_3}{\partial V_3} \cdots \frac{\partial Q_3}{\partial V_n} \\ \vdots \quad \vdots \quad \vdots \quad \vdots \quad \vdots \quad \vdots \quad \vdots \quad \vdots \\ \frac{\partial Q_n}{\partial \delta_2} \frac{\partial Q_n}{\partial \delta_3} \cdots \frac{\partial Q_n}{\partial \delta_n} \frac{\partial Q_n}{\partial V_2} \frac{\partial Q_n}{\partial V_3} \cdots \frac{\partial Q_n}{\partial V_n} \end{bmatrix} \begin{bmatrix} \Delta \delta_2 \\ \Delta \delta_3 \\ \vdots \\ \Delta \delta_n \\ \Delta V_2 \\ \Delta V_3 \\ \vdots \\ \Delta V_n \end{bmatrix} \quad (14)$$

$$\begin{bmatrix} \Delta P \\ \Delta Q \end{bmatrix} = \begin{bmatrix} J_1 & J_2 \\ J_3 & J_4 \end{bmatrix} \begin{bmatrix} \Delta \delta \\ \Delta V \end{bmatrix} \quad (15)$$

Where:
ΔP =Real Power Mismatch
ΔQ = Reactive Power Mismatch
ΔV = Bus Voltage Mismatch
$\Delta \delta$ = Bus Voltage Angle Mismatch
$J_1, J_2, J_3, and\ J_4$ are the elements of Jacobian matrix which are obtained by partial differentiation of the equations (12) and (13) with respect to the state variables δ, V. The off-diagonal and diagonal elements of $J_1, J_2, J_3, and\ J_4$ are as expressed in equations (16) to (23)[33, 34].
The off-diagonal and diagonal elements of J_1:

$$\frac{\partial P_i}{\partial \delta_k} = V_i V_k Y_{ik} \sin(\theta_{ik} + \delta_i - \delta_k); k \neq i \quad (16)$$

$$\frac{\partial P_i}{\partial \delta_i} = -\sum_{k=1}^{n} V_i V_k Y_{ik} \sin(\theta_{ik} + \delta_i - \delta_k); k \neq i \quad (17)$$

The off-diagonal and diagonal elements of J_2:

$$\frac{\partial P_i}{\partial V_k} = V_i V_k Y_{ik} \cos(\theta_{ik} + \delta_i - \delta_k); k \neq i \quad (18)$$

$$\frac{\partial P_i}{\partial V_i} = 2V_i Y_{ii} cos\theta_{ii} + \sum_{k=1}^{n} Y_{ik} V_k \cos(\theta_{ik} + \delta_i - \delta_k); k \neq i \quad (19)$$

The off-diagonal and diagonal elements of J_3:

$$\frac{\partial Q_i}{\partial \delta_k} = -V_i V_k Y_{ik} \cos(\theta_{ik} + \delta_i - \delta_k); k \neq i \quad (20)$$

$$\frac{\partial Q_i}{\partial \delta_i} = \sum_{k=1}^{n} V_i V_k Y_{ik} \cos(\theta_{ik} + \delta_i - \delta_k); k \neq i \quad (21)$$

The off-diagonal and diagonal elements of J_4:

$$\frac{\partial Q_i}{\partial V_k} = V_i Y_{ik} \sin(\theta_{ik} + \delta_i - \delta_k); k \neq i \quad (22)$$

$$\frac{\partial Q_i}{\partial V_i} = 2V_i Y_{ii} sin\theta_{ii} + \sum_{k=1}^{n} Y_{ik} V_k \sin(\theta_{ik} + \delta_i - \delta_k); k \neq i \quad (23)$$

The real and reactive power mismatches at each iteration with new estimates of bus voltage angles and bus voltage magnitude are expressed by equations (24) to (27):

$$\Delta P_i^r = P_i^{spec} - P_i^r \quad (24)$$

$$\Delta Q_i^r = Q_i^{spec} - Q_i^r \quad (25)$$

$$\delta_i^{r+1} = \delta_i^r - \Delta \delta_i^r \quad (26)$$

$V_i^{r+1} = V_i^r - \Delta V_i^r$ (27)

Where:

r = iteration count

ΔP_i^r = Real Power Mismatch at Iteration r

P_i^{spec} = Specified Value of Real Power

P_i^r = Calculated Value of Real Power at Iteration r

ΔQ_i^r = Reactive Power Mismatch at Iteration r

Q_i^{spec} = Specified Value of Reactive Power

Q_i^r = Calculated Value of Reactive Power at Iteration r

δ_i^{r+1} = New Estimate of Bus Voltage Angle at Iteration r + 1

δ_i^r = Calculated Value of Bus Voltage Angle at Iteration r

$\Delta\delta_i^r$ = Bus Voltage Angle Mismatch at Iteration r

V_i^{r+1} = New Estimate of Bus Voltage at Iteration r + 1

V_i^r = Calculated Value of Bus Voltage at Iteration r

ΔV_i^r = Bus Voltage Mismatch at Iteration r

The voltage and reactive power constraints at each bus i are given by equations (28) and (29) respectively:

$V_{imim} \leq V_i \leq V_{imax}$ (28)

$Q_{imim} \leq Q_i \leq Q_{imax}$ (29)

Where:

V_{imim} = Minimum voltage value at bus i

V_{imax} = Maximum voltage value at bus i

Q_{imim} = Minimum reactive power supply at bus i

Q_{imax} = Maximum reactive power supply at bus i

3.TRANSMISSION NETWORK MODEL IN SIMULINK SOFTWARE

The input data for modelling of the transmission network in Simulink software include the bus data that is real and reactive powers of the generator buses, transmission line data (impedance of lines), voltages and load data obtained are presented in Tables 1 and 2 respectively. Fig. 3 also present the block diagram of the Transmission Network. They were used to carry out the simulation analysis.

Table 1: Load data of the test network

Bus Identification		**Bus Loads**		**Transmission Lines Data**				
Name	**No**	**MW**	**MVAR**	**BUS**		**Resistance**	**Reactance**	**Susceptance**
				From	**To**	**R (pu)**	**X (pu)**	**S (PU)**
Swing	1	0.00	0.00	1	2	0.0200	0.0600	0.0300
PV	2	0.00	0.00	1	3	0.0800	0.2400	0.0250
Load	3	20.00	10.00	2	3	0.0600	0.1800	0.0300
PV	4	0.00	0.00	2	4	0.0600	0.1800	0.0200
Load	5	20.00	15.00	2	5	0.0400	0.1200	0.0150
Load	6	50.00	30.00	3	4	0.0100	0.0300	0.0100
Load	7	60.00	40.00	4	5	0.0800	0.2400	0.0250

Table 2: Generator data of the test network

Bus Identification		Voltage	Generator		Reactive Power	
Name	No	Magnitude (pu)	MW	MVAR	Q_{min}	Q_{max}
Swing bus	1	1.06	0.00	0.00	0.00	0.00
PV bus	2	1.045	40.00	0.00	10.00	50.00
PV bus	3	1.03	10.00	0.00	10.00	40.00

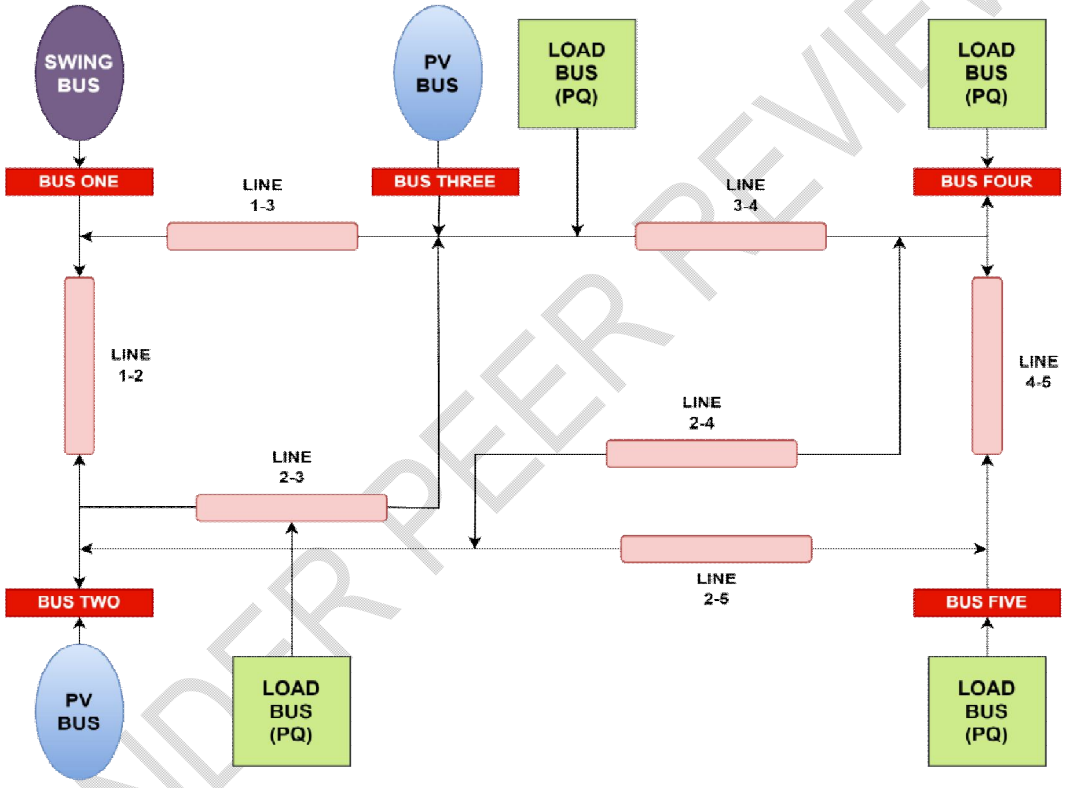

Fig. 3. Block diagram of the transmission network

From the block diagram, Bus 1 (Swing Bus) which serves as a reference point for voltage and phase angle is connected to bus 2 (PV Bus with load) through line 1 and line 2, also to Bus 3 (PV Bus with load) through line 1 and line 3. Bus 2 (PV Bus with load) is connected to bus 1 through line 1 and line 2, also to bus 3 through line 2 and line 3 also to bus 4 (PQ Bus) through line 2 and line 4 and also to bus 5 (PQ Bus) through line 2 and line 5. Bus 3 (PV Bus with load) is connected to bus 1 through line 1 and line 3 also to bus 2 through line 2 and line 3 also to bus 4 (PQ Bus) through line 3 and line 4. Bus 4 (PQ Bus) is linked to Bus 3 via Line 3 and Line 4, and it is also connected to Bus 2 through Line 2 and Line 4. Bus 5 (PQ Bus) is connected to bus 2 through line 2 and line 5 also to bus 4 through line 4 and line 5. This configuration will allow us to perform power flow analysis, especially to understand how the

system operates under different conditions and to investigate the impact of integrating renewable energy sources like solar power into the grid.

3.1Modelling of 3 MW PV Systemin Simulink Software

The specifications outlined in Table 3 were employed to model the PV system accurately.

Table 3 Specifications employed to model the PV system

Number	Component Description	Rating
1	Maximum power ($Pmax$)	213.15W
2	Open circuit voltage (Voc)	36.3V
3	Voltage at maximum power (Vmp)	29V
4	Short circuit current (Isc)	7.84A
5	Current at maximum power (Imp)	7.35A
6	Input voltage	250-300V
7	Output voltage	600V

From table 3 we can calculate the required number of PV array to be connected in series to give the required output power:

$$N_s = \frac{V_{in}}{V_{mp}} = \frac{319}{29} = 11\ series\ string$$

Therefore 11 PV arrays will be required to be connected in series, also to determine the number of arrays to be connected in parallel we can use the following equation:

$$N_p = \frac{P_{out}}{N_S\ X\ P_{max}} \quad (30)$$

Given the required power output P_{out} to be 3MW, series connected string N_s = 11, and Maximum power P_{max}= 213.15W therefore, the number of parallel connected string will be determined as follows:

$$N_p = \frac{3{,}000{,}000}{213.15 * 11} = 1300\ paralle\ string$$

Therefore, 1300 parallel string is required to give the desired output power. The following expression is used to calculate the required resistance:

Given that current $(I) = \frac{power\ output}{voltage}$

$$(I) = \frac{3{,}000{,}000}{319} = 9555\ watts$$

The resistance can be calculated using ohms' law which is express as, $R\frac{V}{I}$

$$R = \frac{319}{9555} = 0.033\Omega$$

The above values were inputted into the appropriate fields in Simulink and visualized using graphical plots, this gives a total power output of 3MW.

4. SIMULATION RESULTS AND DISCUSSION

The graphical models extracted from the PV model are represented in this section, the graphs show the three remarkable points in any solar PV cell that include the open circuit voltage (V_{OC}), the maximum power point (M_{PP}) and the short circuit current (I_{OC}). Table 4 provides an overview of the key parameters required in configuring the simulated solar PV array to supply the desired potential required output power to be integrated into the transmission line:

Table 4: Required Parameters of the Modelled PV Array

Number	Required Parameters	Value
1	Irradiance	1000 W/m^2
2	Number of parallel strings	1300
3	Number of series connected modules per string	11
4	Number of cells per module	60
5	Open circuit voltage (Voc)	36.3V
6	Voltage at maximum power (Vmp)	29V
7	Short circuit current (Isc)	7.84A
8	Current at maximum power (Imp)	7.35A
9	Temperature coefficient of short circuit current (Isc)	0.102^{0}c
10	Temperature coefficient of open circuit voltage (Voc)	-0.36099^{0}c
11	Solar cell maximum power	213.15W
12	Shunt resistance R_{sh} $(ohms)$	313.3991Ω
13	Series resistance R_s $(ohms)$	0.39383Ω
14	Diode idealistic factor	0.98117

The following graphs were extracted while modelling the PV array in Simulink to enable evaluation of the solar characteristics under different operating conditions.

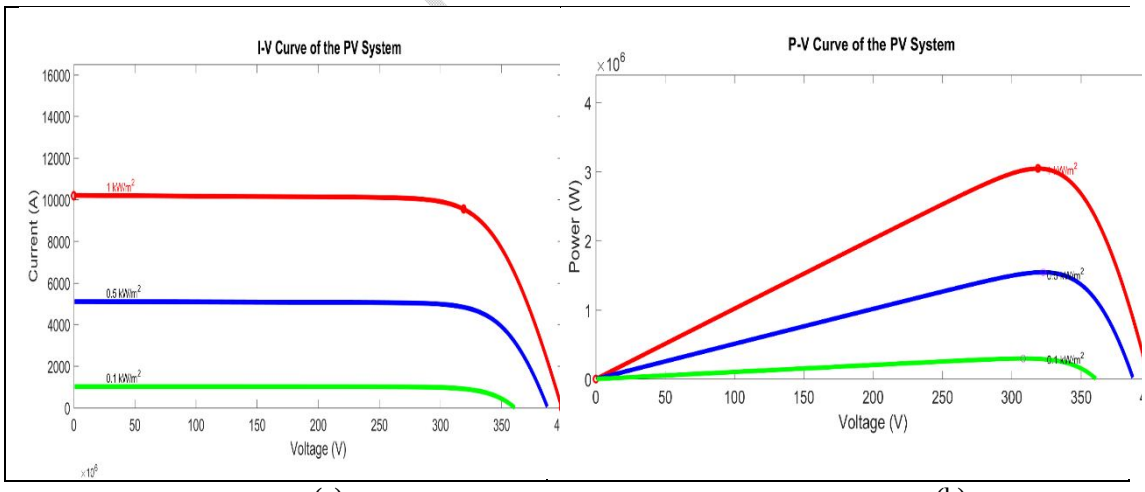

(a) (b)

Fig. 4. (a) Current and voltage relationship of solar PV module. (b) Power and voltage relationship of solar PV module

As seen in Fig. 4. the current, voltage and power relationship of the PV array at different solar irradiance is obtained. Fig. 4. (a) representing the current and voltage relationship of the solar cell at different irradiance level while Fig. 4. (b) presents the relationship between Power and voltage of the solar cell at different irradiance level.

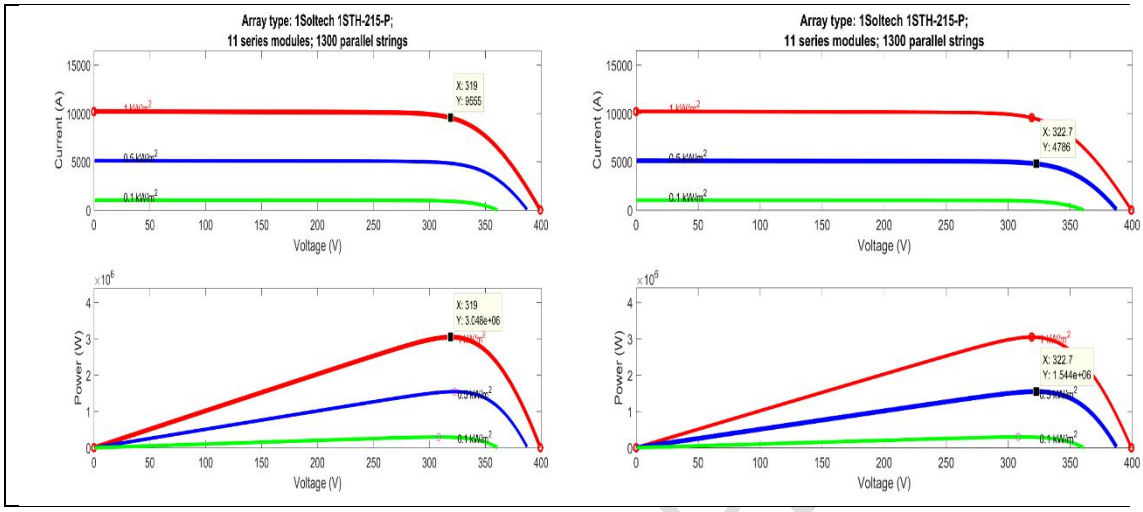

(a) (b)

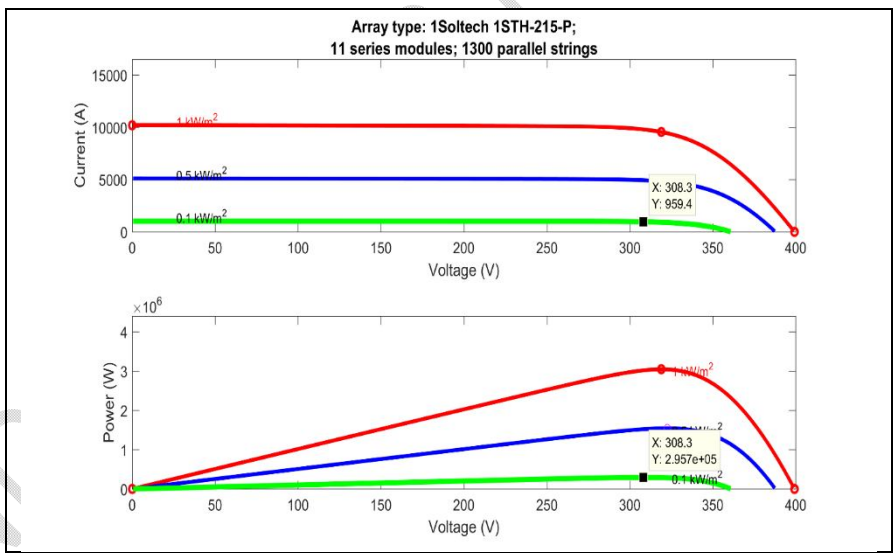

(c)

Fig. 5. (a) PV array specification with 1k W/m^2 irradiance. (b) PV array specified with 0.5k W/m^2 irradiance. (c) PV array specified with 0.1k W/m^2 irradiance

Fig. 5. (a) showed that a total current, voltage, and power of 9555 amps, 319 volts and 3 MW respectively were recorded at 1k W/m^2 irradiance. As seen in Fig. 5. (b), at 0.5 kW/m^2 irradiance the voltage slightly increases to 322.7 volts while current and power reduced to 4786 amps and 1.5 MW respectively. Similarly, Fig. 5. (c) show that at 0.1 kW/m^2 irradiance the voltage, current and power reduced to 308.3 volts, 959.4 amps and 0.29 MW respectively. This result showed that, current and power of the PV array depends on the available of solar irradiance.

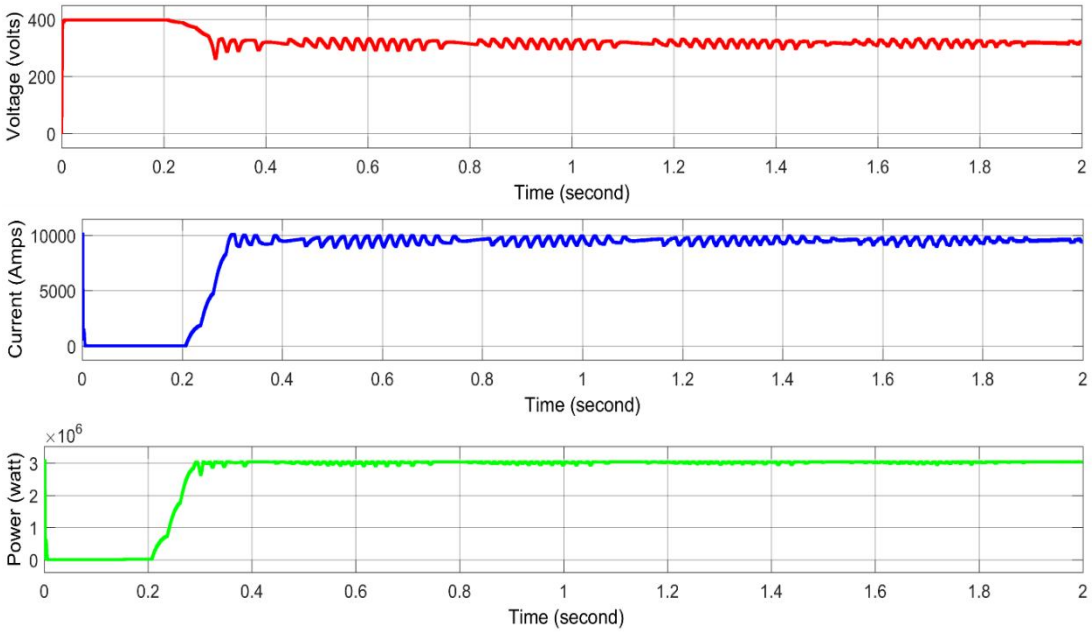

Fig. 6. PV array output current, voltage and power

The generated current of the PV array is shown in Fig. 6. The current was measured at approximately 9555 A. This high current output reflects the PV array's capacity to deliver substantial electrical power to the network, particularly under optimal irradiance conditions. The voltage output from the PV array was observed to be around 319 volts and the output power delivered is approximately 3 MW. This power generation considered to directly supports the grid by enhancing overall power availability and stabilizing voltage across transmission lines.

4.1 Load Flow Analysis Results

The load flow analysis was conducted on the transmission network to examine voltage levels, power flows, and the distribution of real and reactive power across various buses. Each bus in the network has distinct characteristics based on the types of loads and sources connected. table 5 present the load flow analysis result without integration of renewable energy.

Table 5: Load Flow Analysis Result without Renewable Energy Integration

Bus no	Per-Unit Voltage(pu)	Load		Generation		Remark
		MW	Mvar	MW	Mvar	
1	1.0600	0.00	0.00	83.05	7.27	Swing bus
2	0.8302	20.00	10.00	0.00	0.00	Load bus
3	0.8302	0.00	0.00	40.00	41.01	PV bus
4	0.6338	20.00	15.00	0.00	0.00	Load bus
5	0.6338	0.00	0.00	30.00	24.15	PV bus
6	0.5344	50.00	30.00	0.00	0.00	Load bus
7	0.6581	60.00	40.00	0.00	0.00	Load bus
Total		**150.00**	**95.00**	**153.05**	**72.43**	

From table 5, the swing bus is set at 1.060 pu, providing a slightly elevated voltage to compensate for power imbalances across the network. The voltage at bus 2 dropped to 0.8302 pu due to the combined impact of the PQ load and PV source. The drop below 0.9 pu suggests a need for additional voltage support to maintain power quality and stability. At bus 3, the per-unit voltage is 0.6338 pu, reflecting a significant drop caused by high load demand. Bus 4 has the lowest voltage at 0.5344 pu. Such a low voltage is problematic, as it can lead to operational issues, especially for voltage-sensitive equipment, and may destabilize the network. With a voltage of 0.6581 pu, bus 5 also experiences a notable voltage drop due to high load demand. This level, though slightly better than bus 4, still requires improvement to ensure stable operation and efficient power distribution. The total active power loss was also calculated to be 3.05 MW.

4.2 Load Flow Analysis After Solar Renewable Energy Integration

The integration of solar renewable energy into the transmission network was aimed to enhance voltage stability and reduce the load burden on traditional sources. The load flow analysis following this integration at bus 4 yielded the following per-unit voltages, load, and generation values at each bus as shown in table 6.

Table 6: Load Flow Analysis Result with Renewable Energy Integration

Bus no	Per-Unit Voltage(pu)	Load		Generation		Remark
		MW	Mvar	MW	Mvar	
1	1.0600	0.00	0.00	83.05	7.27	Swing bus
2	0.9902	20.00	10.00	0.00	0.00	Load bus
3	0.9902	0.00	0.00	40.00	41.01	PV bus
4	1.0001	20.00	15.00	0.00	0.00	Load bus
5	1.0001	0.00	0.00	30.00	24.15	PV bus
6	1.0100	52.40	15.00	0.00	0.00	Load bus
7	0.9947	60.00	40.00	0.00	0.00	Load bus
Total		**152.40**	**80.00**	**153.05**	**72.43**	

As seen in table 6, the voltage at most buses is now close to or above 1.0 pu, indicating a much-improved voltage profile across the system compared to previous results, where several buses had voltages below 0.8 pu. Some buses with previous voltage drop (e.g., bus 2, bus 3, bus 4, and bus 5) now have increased voltage levels. For example, bus 2 improved from 0.8302 pu to 0.9902 pu, bus 3 improved from 0.6338 pu to 1.0001 pu, bus 4 increased from 0.5344 pu to 1.0100 pu, and bus 5 improved from 0.6581pu to 0.9947 pu. Total active power demand also increased slightly to 152.40 MW (from 150 MW), given a total active power loss to be 0.65 MW. The bar chart in Fig. 7, and 8 shows the summary of per unit voltage and total real power loss.

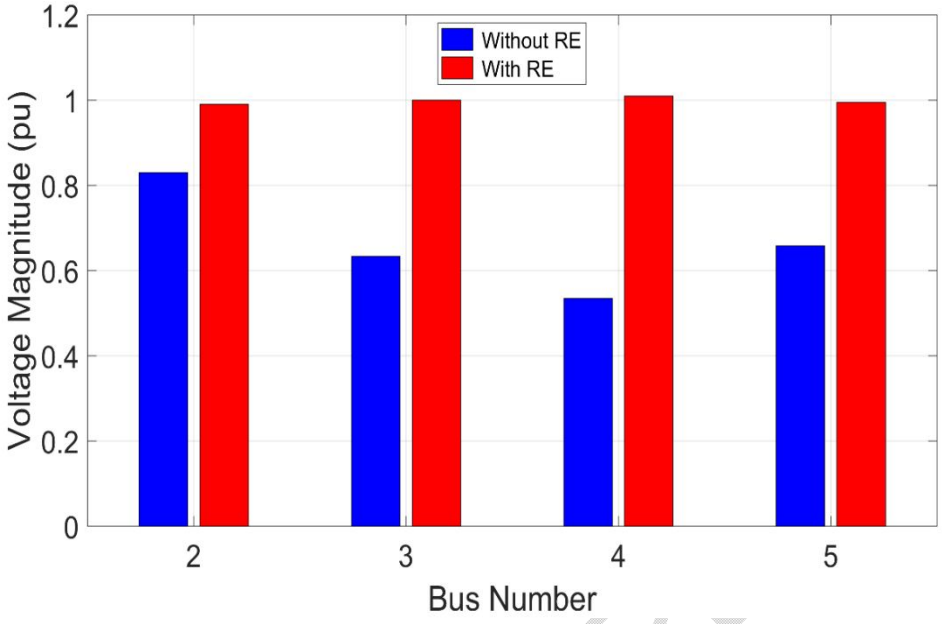

Fig. 7. Bar chart showing the voltage profile without and with RE

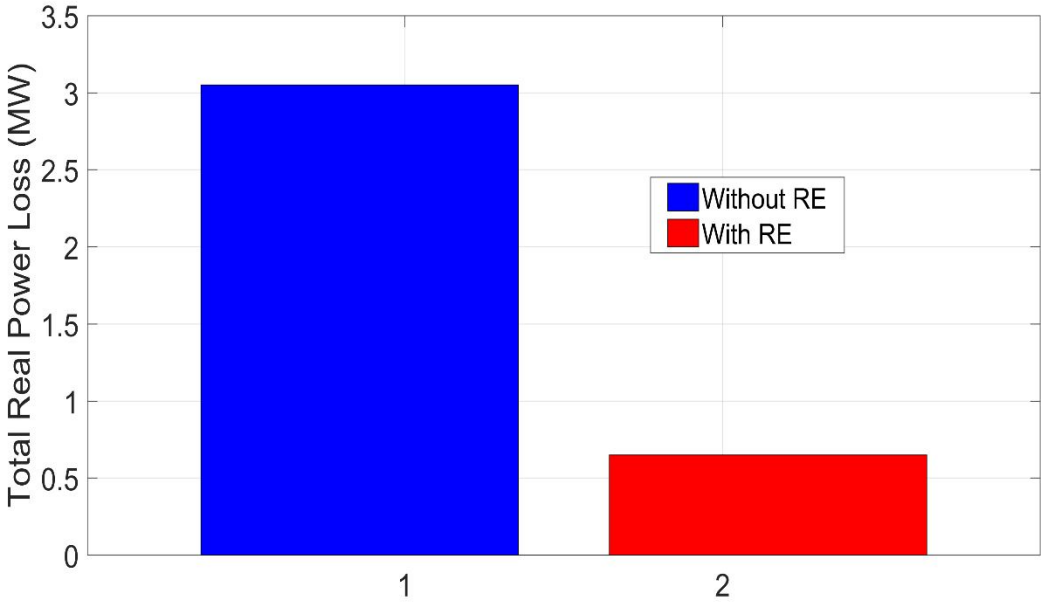

Fig. 8. Bar Chart Showing the Total Active Power Loss without and with RE

From Fig. 7, it was observed that without renewable energy applied to the test network, the voltage magnitudes of four buses, that is, buses 2, 3, 4, and 5, which were respectively of 0.8302, 0.6338, 0.5344 and 0.6581 fell outside of the acceptable limit defined by $0.95 \leq V_i \leq 1.05$ p. u. However, when renewable was incorporated in the test network, the buses whose voltage magnitudes were outside the acceptable limit and some other buses whose voltage magnitudes were already within the acceptable limit had their voltage magnitudes improved.

The voltage magnitudes of buses 2, 3, 4, and 5, respectively improved to 0.9902, 1.0001, 1.0100 and 0.9947. Equally, from Fig. 8, it was observed that the total active power loss on the test network improved with application of renewable energy. The total active power loss which was 3.05 MW without renewable energy reduced to 0.65 MW with renewable energy, giving a 78.33% reduction in total active power loss. These results are indication that integrating a renewable energy in the transmission network is not only capable of improving and maintaining the system's voltage profile within an acceptable limit but will also reduce power loss and in effect improve power transfer capability of the system if applied.

5. CONCLUSIONS

The integration of renewable energy into the Nigerian 330 kV transmission network was explored to assess its potential for improving voltage stability, reducing power losses, and enhancing overall power transfer capability. This research specifically focused on solar renewable energy, using a combination of load flow analysis and simulations to evaluate its impact on the network.Without renewable energy integration, several buses in the test network experienced voltage magnitudes outside the acceptable operational limits, causing potential instability in the system. However, after incorporating solar renewable energy, the voltage magnitudes of key buses improved, bringing them within the desired range of $0.95 \leq V_i \leq 1.05$ per unit. This demonstrated the capacity of renewable energy to enhance voltage stability across the network.Moreover, the study found a substantial reduction in total active power loss, from 3.05 MW to 0.65 MW, representing a 78.33% improvement. This reduction not only highlighted the efficiency benefits of renewable energy integration but also suggested an increase in the power transfer capability of the transmission network.
The research provides important insights into the practical benefits of integrating renewable energy into high-voltage transmission systems, particularly for improving voltage profiles, reducing energy losses, and ensuring efficient power delivery. These findings support the use of renewable energy as a viable solution to the challenges faced by Nigeria's transmission network and can inform future policy, investment, and infrastructure development in the energy sector.

References

[1] "Electricity demand in Nigeria 2000-2023," Google, [Online]. Available: https://www.statista.com/statistics/1306955/electricity-demand-in-nigeria. [Accessed 20 Aug 2024].

[2] A. Aroge, "The Smart Grid and Renewable Energy Integration in Nigeria February, 2014," 2014.

[3] D. R. Patrick, S. W. Fardo and B. W. Fardo, "Electrical power systems technology," River Publishers, 2022.

[4] I. E. Nkan, O. I. Okoro, P. I. Obi, C. C. Awah and U. B. Akuru, "Application of FACTS devices in a multi-machine power system network for transient stability enhancement: A case study of the Nigerian 330kV 48-bus system," in *In 2019 IEEE AFRICON*, 2019.

[5] D. C. Idoniboyeobu, L. S. Braide and H. C. Saaronee, "Improvement of 33KV/11KV Distribution Network at Gboko, Buruku and GumaAgasha in Benue State, Nigeria.Global Scientific Journals, 8(3): 1537-1577," *Global Scientific Journals,* vol. 8, no. 3, pp. 1537-1577, 2020.

[6] F. P. Jameson, I. E. Nkan and E. E. Okpo, "Improvement of power transfer capability of Nigeria national grid with TCSC FACTS controller," *American Journal of Engineering Research (AJER),* vol. 13, no. 1, pp. 37-43, 2024.

[7] C. J. Diji, D. D. Ekpo and C. A. Adadu, "Design of a Biomass Power Plant for a Major

Commercial Cluster in Ibadan-Nigeria," *The International Journal Of Engineering And Science,* vol. 2, no. 3, pp. 23-29, 2013.

[8] R. A. Jokojeje, I. A. Adejumobi, A. O. Mustapha and O. I. Adebisi, "Application of Static synchronous compensator (Statcom) in improving Power System performance: a Case Study of the Nigeria 330 Kv electricity Grid.," *Nigerian Journal of Technology,* vol. 34, no. 3, pp. 564-572, 2015.

[9] R. Sirjani and R. J. Ahmad, "Optimal placement and sizing of distribution static compensator (D-STATCOM) in electric distribution networks," *A review." Renewable and Sustainable Energy Reviews ,* vol. 77 , pp. 688-694., 2017.

[10] I. Nkan, P. Obi, H. Natala and O. Okoro, "Investigation of the transfer capability of the Nigerian 330 kV, 58-bus power system network using FACTS devices," *ELEKTRIKA-Journal of Electrical Engineering,* vol. 22, no. 1, pp. 53-62, 2023.

[11] B. E. Olatunbosun, B. E. Uguru-Okorie and D. A. Ekpo, "Comparison of medical waste generated in selected private and public hospitals in Abeokuta metropolis, Nigeria.," *International Journal of Scientific & Engineering Research,* vol. 5, no. 7, pp. 1441-9, 2014.

[12] A. Zaman, "100% Variable Renewable Energy Power Systems: Survey of Possibilties," Doctoral dissertation, 2018.

[13] D. H. Tungadio and Y. Sun, "Load frequency controllers considering renewable energy integration in power system," 2019.

[14] I. E. Nkan and E. E. Okpo, "Electric power forecasting by the year 2020 using the least square method," *International Journal of Research and Advancement in Engineering Science,* vol. 6, no. 1, pp. 205-215, 2016.

[15] U. B. Akuru, I. E. Onukwube, O. I. Okoro and E. S. Obe, "Towards 100% renewable energy in Nigeria," in *Renewable and Sustainable Energy Reviews*.

[16] R. Cossent, G. Tomás and O. Luis, "Large-scale integration of renewable and distributed generation of electricity in Spain: Current situation and future needs.," *Energy Policy,* vol. 39, no. 12, pp. 8078-8087, 2011.

[17] D. D. EKPO, "Electricity Generation Potential from Municipal Solid Waste in Uyo Metropolis, Nigeria," 2019.

[18] C. J. Diji, D. D. Ekpo and C. A. Adadu, "Exegoenvironmental evaluation of a cement manu-facturing process in Nigeria," *International journal of engineering re-search and development,* vol. 7, pp. 25-32, 2013.

[19] U. O. Innocent, I. E. Nkan and E. E. O. O. I. Okpo, "Predicting the stability behaviour of three-horse power induction motor using eigenvalue method," *Bayero Journal of Engineering and Techcnology (BJET),* vol. 16, no. 2, pp. 66-81, 2021.

[20] B. P. Heard, B. W. Brook, T. M. Wigley and C. J. Bradshaw, "Burden of proof: A comprehensive review of the feasibility of 100% renewable-electricity systems," *Renewable and Sustainable Energy Reviews,,* vol. 76, pp. 1122-1133, 2017.

[21] D. D. Ekpo, C. Diji and A. Offiong, "Environmental degradation and municipal solid waste management in Eket," *International Journal of Engineering Innovations ,* vol. 4, no. 3, pp. 2276-6138, 2012.

[22] H. C. Gils, S. Yvonne, P. Thomas, L. d. T. Diego and H. Dominik, "Integrated modelling of variable renewable energy-based power supply in Europe," *Energy,* vol. 123, pp. 173-188, 2017.

[23] I. K. Okakwu and E. A. Ogujor, "Enhancement of transient stability of the Nigeria 330 kV transmission network using fault current limiter.," *Journal of Power and Energy Engineering,,* vol. 5, no. 9, pp. 92-103, 2017.

[24] E. A. Nyiekaa, G. S. Ape and J. Agber, "Power Transmission Enhancement of the North

Central Nigeria 330 kV Network through Optimal Placement and Sizing of TCSC and UPFC Using Whale Optimization Algorithm," *IOSR Journal of Electrical and Electronics Engineering,* vol. 17, no. 5, pp. 50-60, 2022.

[25] M. R. Patel and O. Beik, "Wind and solar power systems: design, analysis, and operation," CRC press, 2021.

[26] U. O. Innocent, I. E. Nkan, E. E. Okpo and O. I. Okoro, "Dynamic response evaluation of a separately excited dc motor," *Nigeria Journal of Engineering,* vol. 28, no. 2, pp. 56-61, 2021.

[27] E. N. Vincent and S. D. Yusuf, "Integrating renewable energy and smart grid technology into the Nigerian electricity grid system," in *Smart Grid and Renewable Energy*, 2014.

[28] I. K. Okakwu and E. A. Ogujor, "Enhancement of transient stability of the Nigeria 330 kV transmission network using fault current limiter.," *Journal of Power and Energy Engineering,* vol. 5, no. 9, pp. 92-103, 2017.

[29] O. D. Atoki, B. Adebanji, A. Adegbemile, E. T. Fasina and O. D. Akindele, "Sustainable Energy Growth in Nigeria: The role of Grid-connected hybrid power system," *NTERNATIONAL JOURNAL OF SCIENTIFIC & TECHNOLOGY RESEARCH,* vol. 9, no. 9, pp. 274-281, 2020.

[30] E. A. Williams, M. O. Raimi, E. I. Yarwamara and O. Modupe, "Renewable energy sources for the present and future: an alternative power supply for Nigeria," *Energy and Earth Science,* vol. 2, no. 2, 2019.

[31] B. Adebanji, A. Ojo, T. Fasina, S. Adeleye and J. Abere, "Integration of renewable energy with smart grid application into the Nigeria's power network: Issues, challenges and Opportunities," *European Journal of Engineering and Technology Research,* vol. 7, no. 3, pp. 18-24, 2022.

[32] M. Ghiasi, "A detailed study for load flow analysis in distributed power system," *International Journal of Industrial Electronics Control and Optimization ,* vol. 1, no. 2, pp. 153-160, 2018.

[33] J. B. Gupta, A Course in Power Systems, New Delhi, India: S.K. Kataria and Sons Publisher, Gupta, J.B. (2011). A Course in Power Systems. .

[34] D. P. Kothari and I. J. Nagrath, Power system engineering,, Tata McGraw-Hill Publishing Company, 2008.

[35] A. S. Pabla, Electric power distribution., New Delhi, India: Tata McGraw-Hill, 2011.